Inorganic Chemistry
Article

Inorg. Chem. **2011**, *50*, 1265–1274 **1265**
DOI: 10.1021/ic101782v

Aggregation of $[Au(CN)_4]^-$ Anions: Examination by Crystallography and ^{15}N CP-MAS NMR and the Structural Factors Influencing Intermolecular Au···N Interactions

Andrew R. Geisheimer,[†] John E. C. Wren,[‡] Vladimir K. Michaelis,[‡] Masayuki Kobayashi,[†,§] Ken Sakai,[§] Scott Kroeker,*[,‡] and Daniel B. Leznoff*[,†]

[†]*Department of Chemistry, Simon Fraser University, 8888 University Drive, Burnaby, British Columbia, Canada V5A 1S6,* [‡]*Department of Chemistry, University of Manitoba, Winnipeg, Manitoba, R3T 2N2 Canada, and* [§]*Department of Chemistry, Faculty of Science, Kyushu University, Hakozaki 6-10-1, Higashi-ku, Fukuoka, 812-8581 Japan*

Received September 1, 2010

To investigate the factors influencing the formation of intermolecular Au···NC interactions between $[Au(CN)_4]^-$ units, a series of $[cation]^{n+}[Au(CN)_4]_n$ double salts was synthesized, structurally characterized and probed by IR and $^{15}N\{^1H\}$ CP-MAS NMR spectroscopy. Thus, $[^nBu_4N][Au(CN)_4]$, $[AsPh_4][Au(CN)_4]$, $[N(PPh_3)_2][Au(CN)_4]$, $[Co(1,10\text{-phenanthroline})_3][Au(CN)_4]_2$, and $[Mn(2,2';6',2''\text{-terpyridine})_2][Au(CN)_4]_2$ show $[Au(CN)_4]^-$ anions that are well-separated from one another; no Au−Au or Au···NC interactions are present. *trans*-$[Co(1,2\text{-diaminoethane})_2Cl_2]$-$[Au(CN)_4]$ forms a supramolecular structure, where *trans*-$[Co(en)_2Cl_2]^+$ and $[Au(CN)_4]^-$ ions are found in separate layers connected by Au−CN···H−N hydrogen-bonding; weak Au···NC coordinate bonds complete octahedral Au(III) centers, and support a 2-D (4,4) network motif of $[Au(CN)_4]^-$-units. A similar structure-type is formed by $[Co(NH_3)_6][Au(CN)_4]_3\cdot(H_2O)_4$. In $[Ni(1,2\text{-diaminoethane})_3][Au(CN)_4]_2$, intermolecular Au···NC interactions facilitate formation of 1-D chains of $[Au(CN)_4]^-$ anions in the supramolecular structure, which are separated from one another by $[Ni(en)_3]^{2+}$ cations. In [1,4-diazabicyclo[2.2.2]octane-H][$Au(CN)_4$], the monoprotonated amine cation forms a hydrogen-bond to the $[Au(CN)_4]^-$ unit on one side, while coordinating to the axial sites of the gold(III) center through the unprotonated amine on the other, thereby generating a 2-D (4,4) net of cations and anions; an additional, uncoordinated $[Au(CN)_4]^-$-unit lies in the central space of each grid. This body of structural data indicates that cations with hydrogen-bonding groups can induce intermolecular Au···NC interactions, while the cationic charge, shape, size, and aromaticity have little effect. While the ν_{CN} values are poor indicators of the presence or absence of N-cyano bridging between $[Au(CN)_4]^-$-units (partly because of the very low intensity of the observed bands), $^{15}N\{^1H\}$ CP-MAS NMR reveals well-defined, ordered cyanide groups in the six diamagnetic compounds with chemical shifts between 250 and 275 ppm; the resonances between 260 and 275 ppm can be assigned to C-bound terminal ligands, while those subject to CN···H−N bonding resonate lower, around 250−257 ppm. The ^{15}N chemical shift also correlates with the intermolecular Au···N distances: the shortest Au−N distances also shift the ^{15}N peak to lower frequency. This provides a real, spectroscopically measurable electronic effect associated with the crystallographic observation of intermolecular Au···NC interactions, thereby lending support for their viability.

Introduction

The field of metal−organic coordination polymers has received a great deal of focused research attention recently.[1,2] This is largely because of the wide range of properties observed for these materials, including magnetic,[3−7] luminescent,[8] gas storage,[9,10] birefringent,[11,12]

*To whom correspondence should be addressed. E-mail: dleznoff@sfu.ca (D.B.L.); scott_kroeker@umanitoba.ca (S.K.). Tel: 1-778-782-4887 (D.B.L.); 1-204-474-9335 (S.K.). Fax: 1-778-782-3765 (D.B.L.); 1-204-474-7608 (S.K.).

(1) Janiak, C. *Dalton Trans.* **2003**, 2781–2804.
(2) Czaja, A. U.; Trukhan, N.; Muller, U. *Chem. Soc. Rev.* **2009**, *38*, 1284–1293.
(3) Batten, S. R.; Murray, K. S. *Coord. Chem. Rev.* **2003**, *246*, 103–130.
(4) Kurmoo, M. *Chem. Soc. Rev.* **2009**, *38*, 1353–1379.
(5) Lescouezec, R.; Toma, L. M.; Vaissermann, J.; Verdaguer, M.; Delgado, F. S.; Ruiz-Perez, C.; Lloret, F.; Julve, M. *Coord. Chem. Rev.* **2005**, *249*, 2691–2729.
(6) Miller, J. S. *MRS Bull.* **2000**, *25*, 60–64.
(7) Shatruk, M.; Avendano, C.; Dunbar, K. R. *Prog. Inorg. Chem.* **2009**, *56*, 155–334.
(8) Allendorf, M. D.; Bauer, C. A.; Bhakta, R. K.; Houk, R. J. T. *Chem. Soc. Rev.* **2009**, *38*, 1330–1352.
(9) James, S. L. *Chem. Soc. Rev.* **2003**, *32*, 276–288.
(10) Murray, L. J.; Dinca, M.; Long, J. R. *Chem. Soc. Rev.* **2009**, *38*, 1294–1314.

Published on Web 01/26/2011

and vapochromic[13−15] properties. Many of these properties depend on the formation of an ordered, highly dimensional structure; as a result, an important goal in this field is to gain an understanding of the factors that govern the supramolecular structure adopted for a particular coordination polymer.[16−19] Such control and knowledge would greatly enhance the ability to design coordination polymers to exhibit properties of interest.

This goal is often challenging because of the multitude of factors that control packing of a solid-state material during crystallization. Weak forces such as hydrogen bonding, $\pi-\pi$ interactions, weak coordinate bonds, and metallophilic interactions collectively influence the structure of a coordination polymer.[20,21] With the same order of magnitude of strength as a hydrogen-bond, Au(I) and Ag(I) metallophilic interactions have been studied widely.[22−26] Heterobimetallic coordination polymers based on $[M(CN)_2]^-$ (M = Ag, Au) have been able to increase structural dimensionality through such metallophilic interactions, resulting in dramatically different structures than would occur without the interactions.[20] It is known that aurophilic interactions in $[Au(CN)_2]^-$ salts are favored by cations able to participate in hydrogen bonding, either as complex cations or protonated organic heterocycles.[27−29]

Metallophilicity has also been observed in cyanometallates containing d^8 metals such as $[Pt(CN)_4]^{2-}$, where metallophilic interactions have strongly influenced some structures.[14,15,20,30−32] However, for the isoelectronic d^8 Au(III) analogue, $[Au(CN)_4]^-$, no Au(III)−Au(III) interactions have been observed in previously reported $[Au(CN)_4]^-$ complexes and coordination polymers; these include several heterobimetallic coordination polymers with Ni(II) and Cu(II) metal centers as well as with hydroxide-bridged Cu(II) dimers.[33−36] Instead, weak Au···NC-Au coordinate bonds from terminal N-cyano units to vacant axial sites of adjacent Au(III) atoms were observed in several cases, resulting in five- or six-coordinate Au(III) centers.[33−36] However, a systematic study has not been previously performed to investigate whether or not certain conditions favor the formation of these weak Au···NC coordinate bonds. The knowledge of whether self-aggregation is observed for $[Au(CN)_4]^-$ and if so, how it is induced, would be invaluable in the design of coordination polymers incorporating $[Au(CN)_4]^-$.

In this light, we prepared a series of $[cation]^{n+}[Au(CN)_4]_n$ double salts, with the cations judiciously chosen to span a range of cation charge, shape, aromaticity, and ability to participate in hydrogen bonding; as a result, the effect of these factors on the self-aggregation of $[Au(CN)_4]^-$ anions could be examined. In addition to the structural studies, selected compounds were analyzed by solid-state ^{15}N CP-MAS NMR spectroscopy in order to probe if a shift in the characteristic ^{15}N resonance of the Au-CN moiety was observed upon N-cyano coordination to Au(III) via the aforementioned interanionic Au···NC interactions. Overall, this study provides spectroscopic support for the existence of and insight into this weak interaction.

Experimental Section

General Experimental Procedures. All reactions were performed in air using purified solvents. *trans*-$[Co(en)_2Cl_2]Cl$ (en = 1,2-diaminoethane) was prepared as previously reported.[37] [Hdabco]Cl (dabco = 1,4-diazabicyclo[2.2.2]octane) was prepared by stoichiometric addition of HCl to dabco in water, followed by solvent evaporation. All other reagents were used as received from commercial sources. Infrared spectra were measured as KBr pellets on a Thermo-Nicolet Nexus 670 FT-IR spectrometer with a resolution of 1 cm^{-1}. Microanalyses (C, H, N) were performed at Simon Fraser University by Mr. Frank Haftbaradaran using a Carlo Erba (Model 1106) CHN analyzer.

Caution! *Although difficulties have not been experienced, perchlorate salts are potentially explosive and thus should be handled with care and used only in small quantities.*

Synthesis of $[^nBu_4N][Au(CN)_4]$ (1). Dropwise addition of tetrabutylammonium bromide, $[^nBu_4N]Br$, (0.039 g, 0.12 mmol) in a 2 mL aqueous solution to a 2 mL aqueous solution of potassium tetracyanoaurate, $KAu(CN)_4$, (0.037 g, 0.11 mmol) resulted in a colorless solution. Slow evaporation of the solution yielded X-ray quality, colorless crystals of $[^nBu_4N][Au(CN)_4]$ after two weeks, which were vacuum-filtered and air-dried. Yield: 0.043 g, 72%. Anal. Calcd. for $C_{20}H_{36}N_5Au$: C 44.20%, H 6.68%, N 12.89%. Found: C 44.31%, H 6.68%, N 13.00%. IR (KBr): 2996(m) 2970(st), 2959(st), 2930(m), 2874(m), 2832(w), 2735(w), ν(CN): **2183(vw)**, 1488(st), 1467(m), 1382(m), 1186(w), 1152(mw), 1106(mw), 1053(mw), 1026(m), 879(m), 747(m) cm^{-1}.

Polycrystalline $[^nBu_4N][Au(CN)_4]$ can also be prepared with an identical IR spectrum and elemental analysis by mixing a 40 mL aqueous solution of $[^nBu_4N]Br$ (1.072 g, 3.33 mmol) with a 60 mL aqueous solution of $KAu(CN)_4$ (1.000 g, 2.94 mmol). A white precipitate of $[^nBu_4N][Au(CN)_4]$ forms immediately and was isolated by vacuum filtration. Yield: 1.484 g, 92.9%.

Synthesis of $[AsPh_4][Au(CN)_4]$ (2). A 4 mL 50% v/v methanol/water solution of tetraphenylarsonium chloride, $[AsPh_4]Cl$,

(11) Katz, M. J.; Kaluarachchi, H.; Batchelor, R. J.; Bokov, A. A.; Ye, Z. G.; Leznoff, D. B. *Angew. Chem., Int. Ed.* **2007**, *46*, 8804–8807.
(12) Katz, M. J.; Leznoff, D. B. *J. Am. Chem. Soc.* **2009**, *131*, 18435–18444.
(13) Lefebvre, J.; Batchelor, R. J.; Leznoff, D. B. *J. Am. Chem. Soc.* **2004**, *126*, 16117–16125.
(14) Buss, C. E.; Anderson, C. E.; Pomije, M. K.; Lutz, C. M.; Britton, D.; Mann, K. R. *J. Am. Chem. Soc.* **1998**, *120*, 7783–7790.
(15) Drew, S. M.; Janzen, D. E.; Buss, C. E.; MacEwan, D. I.; Dublin, K. M.; Mann, K. R. *J. Am. Chem. Soc.* **2001**, *123*, 8414–8415.
(16) Batten, S. R.; Murray, K. S. *Aust. J. Chem.* **2001**, *54*, 605–609.
(17) Batten, S. R.; Robson, R. *Angew. Chem., Int. Ed.* **1998**, *37*, 1460–1494.
(18) Dunbar, K. R.; Heintz, R. A. *Prog. Inorg. Chem.* **1997**, *45*, 283–391.
(19) Kitagawa, S.; Kitaura, R.; Noro, S. *Angew. Chem., Int. Ed.* **2004**, *43*, 2334–2375.
(20) Katz, M. J.; Sakai, K.; Leznoff, D. B. *Chem. Soc. Rev.* **2008**, *37*, 1884–1895.
(21) Roesky, H. W.; Andruh, M. *Coord. Chem. Rev.* **2003**, *236*, 91–119.
(22) Bardaji, M.; Laguna, A. *J. Chem. Educ.* **1999**, *76*, 201–203.
(23) Pyykkö, P. *Angew. Chem., Int. Ed.* **2004**, *43*, 4412–4456.
(24) Pyykkö, P. *Chem. Soc. Rev.* **2008**, *37*, 1967–1997.
(25) Schmidbaur, H. *Gold Bull.* **2000**, *33*, 3–10.
(26) Schmidbaur, H.; Schier, A. *Chem. Soc. Rev.* **2008**, *37*, 1931–1951.
(27) Pham, D. M.; Rios, D.; Olmstead, M. M.; Balch, A. L. *Inorg. Chim. Acta* **2005**, *358*, 4261–4269.
(28) Stender, M.; Olmstead, M. M.; Balch, A. L.; Rios, D.; Attar, S. *Dalton Trans.* **2003**, 4282–4287.
(29) Stender, M.; White-Morris, R. L.; Olmstead, M. M.; Balch, A. L. *Inorg. Chem.* **2003**, *42*, 4504–4506.
(30) Pyykkö, P. *Chem. Rev.* **1997**, *97*, 597–636.
(31) Doerrer, L. H. *Comm. Inorg. Chem.* **2008**, *29*, 93–127.
(32) Angle, C. S.; Woolard, K. J.; Kahn, M. I.; Golen, J. A.; Rheingold, A. L.; Doerrer, L. H. *Acta Crystallogr. C* **2007**, *63*, M231–M234.
(33) Katz, M. J.; Kaluarachchi, H.; Batchelor, R. J.; Schatte, G.; Leznoff, D. B. *Cryst. Growth Des.* **2007**, *7*, 1946–1948.
(34) Katz, M. J.; Aguiar, P. M.; Batchelor, R. J.; Bokov, A. A.; Ye, Z.-G.; Kroeker, S.; Leznoff, D. B. *J. Am. Chem. Soc.* **2006**, *126*, 3669–3676.
(35) Shorrock, C. J.; Jong, H.; Batchelor, R. J.; Leznoff, D. B. *Inorg. Chem.* **2003**, *42*, 3917–3924.
(36) Vitoria, P.; Muga, I.; Gutierrez-Zorrilla, J. M.; Luque, A.; Roman, P.; Lezama, L.; Zuniga, F. J.; Beitia, J. I. *Inorg. Chem.* **2003**, *42*, 960–969.
(37) Bailar, J. C. *Inorg. Synth.* **1946**, *2*, 222–225.

(0.055 g, 0.12 mmol) was added to a 2 mL aqueous solution of $KAu(CN)_4$ (0.036 g, 0.11 mmol). Slow evaporation of the solution yielded colorless, X-ray quality crystals of $[AsPh_4][Au(CN)_4]$ after 10 days, which were vacuum-filtered and air-dried. Yield: 0.044 g, 92%. Anal. Calcd. for $C_{28}H_{20}N_4AsAu$: C 49.14%, H 2.95%, N 8.19%. Found: C 49.13%, H 2.88%, N 8.29%. IR (ATR): 3160(w), 3085(w), 3060(w), 3026(w), 2658(w), 2998(w), ν(CN): **2192(vw)**, **2180(vw)**, 1558(w), 1484(m), 1439(st), 1341(mw), 1310(mw), 1189(mw), 1162(w), 1081(st), 1023(mw), 997(st), 922(w), 843(w) cm^{-1}.

Synthesis of $[N(PPh_3)_2][Au(CN)_4]$ (3). Dropwise addition of bis(triphenylphosphine)iminium chloride, $[N(PPh_3)_2]Cl$, (0.063 g, 0.11 mmol) in a 6 mL 67% v/v methanol/water solution to a 2 mL aqueous solution of $KAu(CN)_4$ (0.036 g, 0.11 mmol) resulted in a white precipitate, which was dissolved upon further addition of 20 mL methanol. X-ray quality colorless crystals of $[N(PPh_3)_2][Au(CN)_4]$ formed during slow evaporation of the solution (for about two weeks); they were then vacuum-filtered and air-dried. Yield: 0.034 g, 54%. Anal. Calcd. for $C_{40}H_{30}N_5AuP_2$: C 57.22%, H 3.60%, N 8.34%. Found: C 57.22%, H 3.46%, N 8.20%. IR (ATR): 3060(w), 3017(w), 2995(w), ν(CN): **2179(vw)**, 1588(mw), 1480(mw), 1438(m), 1334(m), 1302(m), 1181(mw), 1159(w), 1114(st), 998(m), 968(w), 928(w), 854(w), 753(m), 721(st), 691(st) cm^{-1}.

Synthesis of $[Co(phen)_3][Au(CN)_4]_2$ (4). A 2 mL 50% v/v methanol/water solution of 1,10-phenanthroline (phen) (0.036 g, 0.18 mmol) was added to a 3 mL 50% v/v methanol/water solution of cobalt(II) perchlorate, $Co(ClO_4)_2 \cdot 6H_2O$, (0.023 g, 0.063 mmol) resulting in an orange solution. A 10 mL 50% v/v methanol/water solution of $KAu(CN)_4$ (0.068 g, 0.20 mmol) was then added to the solution, which resulted in formation of orange crystals of $[Co(phen)_3][Au(CN)_4]_2$ after 1 day, which were then vacuum-filtered and air-dried. Yield: 0.055 g, 73%. Anal. Calcd. for $C_{34}H_{24}N_{14}Au_2Co$: C 43.98%, H 2.01%, N 16.32%. Found: C 43.88%, H 1.78%, N 15.96%. IR (KBr): 3436(m), 3128(w), 3067(m), 3020(w), 2943(w), 2836(w), ν(CN): **2199(w)**, **2190(w)**, **2185(w)**, **2180(w),** 1626(m), 1587(m), 1519(st), 1426(st), 1343(m), 1225(m), 1144(m), 1104(m), 1024(w), 847(st), 786(m), 725(st), 644(m), 473(m), 458(st), 419(st) cm^{-1}.

Synthesis of $[Mn(terpy)_2][Au(CN)_4]_2$ (5). A 3 mL 50% v/v methanol/water solution of 2,2′;6′,2″-terpyridine (terpy) (0.024 g, 0.10 mmol) was added to a 2 mL 50% v/v methanol/water solution of manganese(II) chloride, $MnCl_2 \cdot 6H_2O$, (0.019 g, 0.052 mmol) resulting in a yellow solution. A 2 mL aqueous solution of $KAu(CN)_4$ (0.069 g, 0.20 mmol) was then added to the solution without any color change. The yellow solution was allowed to slowly evaporate and yellow, X-ray quality crystals of $[Mn(terpy)_2][Au(CN)_4]_2$ were deposited after six days, which were then vacuum-filtered and air-dried. Yield: 0.024 g, 43%. Anal. Calcd. for $C_{38}H_{22}N_{14}Au_2Mn$: C 40.62%, H 1.97%, N 17.45%. Found: C 40.62%, H 1.86%, N 17.07%. IR (KBr): 3113(w), 3062(w), 3054(w), 3031(w), 3021(w), ν(CN): **2188(w)**, 1572(m), 1595(st), 1475(m), 1450(st), 1318(m), 1248(m), 1162(m), 1115(m), 1108(m), 1099(st), 1086(st), 1014(m), 775(st), 651(m), 624(m), 458(st) cm^{-1}.

Synthesis of *trans*-$[Co(en)_2Cl_2][Au(CN)_4]$ (6). A 5 mL 80% v/v methanol/water solution of *trans*-(bis-ethylenediamine) cobalt-(III) chloride, *trans*-$[Co(en)_2Cl_2]Cl$, (0.030 g, 0.11 mmol) was added to a 5 mL 80% v/v methanol/water solution of $KAu(CN)_4$ (0.035 g, 0.10 mmol). The solution was covered with parafilm. After four days, X-ray quality, green crystals of *trans*-$[Co(en)_2Cl_2][Au(CN)_4]$ had formed, and were vacuum-filtered and air-dried. Yield: 0.030 g, 53%. Anal. Calcd. for $C_8H_{16}N_8AuCl_2Co$: C 17.44%, H 2.93%, N 20.33%. Found: C 17.65%, H 2.58%, N 20.17%. IR (KBr): 3443(m), 3301(st), 3281(st), 3237(st), 3135(m), 3126(m), 3001(w), 2986(w), 2959-(mw), ν(CN): **2186(mw)**, 1584(st), 1450(w), 1282(m), 1218(st), 1124(st), 1054(st), 1003(m), 794(w), 589(m) cm^{-1}.

Synthesis of $[Ni(en)_3][Au(CN)_4]_2$ (7). To an 2 mL aqueous solution of nickel(II) perchlorate, $Ni(ClO_4)_2 \cdot 6H_2O$, (0.035 g, 0.096 mmol) 3 mL of an aqueous ethylenediamine (en) stock solution (0.1 M, 0.3 mmol) was added, resulting in a purple solution. A 2 mL aqueous solution of $KAu(CN)_4$ (0.066 g, 0.19 mmol) was added to this solution, which did not cause a change in color or formation of a precipitate; the resultant solution was covered with parafilm. After four days, large, purple, X-ray quality crystals of $[Ni(en)_3][Au(CN)_4]_2$ were recovered by vacuum-filtration and subsequently air-dried. Yield: 0.047 g, 58%. Anal. Calcd. for $C_{14}H_{24}N_{14}Au_2Ni$: C 19.99%, H 2.88%, N 23.32%. Found: C 20.30%, H 2.69%, N 23.57%. IR (ATR): 3341(m), 3291(m), 2960(w), 2895(w) ν(CN): **2185(w)**, **2176(w)**, 1604(m), 1579(m), 1467(w), 1327(w), 1286(w), 1098(m), 1023(st), 967(st) cm^{-1}.

Synthesis of $[Co(NH_3)_6][Au(CN)_4]_3 \cdot 4H_2O$ (8). A 3 mL aqueous solution of hexaamminecobalt(III) chloride, $[Co(NH_3)_6]Cl_3$, (0.026 g, 0.14 mmol) was added to a 4 mL aqueous solution of $KAu(CN)_4$ (0.102 g, 0.300 mmol), which did not alter the color of the initial orange solution. The solution was covered with parafilm and yielded orange, X-ray quality crystals of $[Co(NH_3)_6][Au(CN)_4]_3 \cdot 4H_2O$ after five weeks, which were then vacuum-filtered and air-dried. Yield: 0.065 g, 57%. Anal. Calcd. for $C_{12}H_{26}N_{18}Au_3CoO_4$: C 12.68%, H 2.31%, N 22.19%. Found: C 12.87%, H 2.06%, N 21.91%. IR (KBr): 3653(m), 3644(m), 3229(s,br), 3174(s,br), ν(CN): **2191(m)**, **2189(m)**, 1600(st), 1349(m), 1325(st), 1259(w), 987(w), 822(st), 473(m), 458(m) cm^{-1}.

Synthesis of $[Hdabco][Au(CN)_4]$ (9). Adding a 3 mL aqueous solution of [Hdabco]Cl (0.032 g, 0.22 mmol) to a 5 mL aqueous solution $KAu(CN)_4$ (0.068 g, 0.20 mmol) resulted in a colorless solution. The solution was covered with parafilm and colorless X-ray quality crystals of $[Hdabco][Au(CN)_4]$ were deposited, which were filtered and air-dried. Retention of the filtrate and further slow evaporation yielded additional crystals of $[Hdabco][Au(CN)_4]$. Yield: 0.049 g, 59%. Anal. Calcd. for $C_{10}H_{13}N_6Au$: C 29.00%, H 3.16%, N 20.29%. Found: C 29.14%, H 3.00%, N 19.83%. IR (KBr): 3054(w), 2958(w), 2890(w), 2678(w), ν(CN): **2196(w)**, **2184(w)**, **2175(w),** 1461(m), 1326(st), 1175(st), 1088(st), 1057(st), 1014(st), 941(m), 837(m), 798(st), 772(m), 626(st), 602(st), 458(m) cm^{-1}.

X-ray Crystallographic Analysis. Crystallographic data for all compounds are collected in Table 1. X-ray crystallographic analysis was performed by mounting crystals onto glass fibers using epoxy adhesive and then placing them into a cold nitrogen stream. The diffraction data was collected using a Bruker SMART APEX II CCD area detector diffractometer positioned 6.0 cm from the crystal. The X-ray source was a monochromated Mo Kα radiation (λ = 0.71073 Å) from a rotating anode with a mirror focusing apparatus operated at 1.2 kW (50 kV, 24 mA). The frames were collected with a scan width of 0.5° in ω and were integrated with the Bruker SAINT software. Corrections for absorption were made by SADABS.

The structure of each compound was solved using the Sir 92 routine and expanded using Fourier techniques within the CRYSTALS[38] software package. Hydrogen atoms were placed geometrically, oriented with probable hydrogen bonds, and refined with a riding model to link the shifts of the respective carbon and nitrogen atoms. The crystal of **6** was of poor quality and twinned and was therefore analyzed using twinning deconvolution software. Diagrams were made using Ortep-3 (version 2.02)[39] and POV-Ray (version 3.6.0).[40]

Nitrogen-15 CP MAS NMR. ^{15}N $\{^1H\}$ cross-polarization (CP) magic-angle spinning (MAS) NMR was acquired on a

(38) Betteridge, P. W.; Carruthers, J. R.; Cooper, R. I.; Prout, K.; Watkin, D. J. *J. Appl. Crystallogr.* **2003**, *36*, 1487–1487.
(39) Farrugia, L. J. *J. Appl. Crystallogr.* **1997**, *5*, 565–565.
(40) Fenn, T. D.; Ringe, D.; Petsko, G. A. *J. Appl. Crystallogr.* **2003**, *36*, 944–947.

Table 1. Crystallographic Data for Complexes **1**−**5**

	[^{n}Bu$_4$N][Au(CN)$_4$] (**1**)	[AsPh$_4$][Au(CN)$_4$] (**2**)	[N(PPh$_3$)$_2$][Au(CN)$_4$] (**3**)	[Co(phen)$_3$][Au(CN)$_4$]$_2$ (**4**)	[Mn(terpy)$_2$][Au(CN)$_4$]$_2$ (**5**)
empirical formula	$C_{20}H_{36}N_5Au$	$C_{28}H_{20}N_4AsAu$	$C_{40}H_{30}N_5AuP_2$	$C_{44}H_{24}N_{14}Au_2Co$	$C_{38}H_{22}N_{14}Au_2Mn$
formula weight	507.47	684.38	839.63	1201.64	1123.55
crystal system	monoclinic	triclinic	monoclinic	triclinic	triclinic
space group	$P2_1/n$	$P\bar{1}$	$P2_1/c$	$P\bar{1}$	$P\bar{1}$
a (Å)	14.6965(6)	10.5193(9)	16.7592(5)	11.2733(3)	12.925(3)
b (Å)	8.4684(3)	10.5990(9)	14.6440(4)	11.3956(3)	13.158(4)
c (Å)	19.6174(8)	12.7155(11)	15.6117(4)	16.4575(4)	13.497(4)
α (deg)	90	96.057(4)	90	78.6460(10)	76.64(3)
β (deg)	105.485(2)	103.596(4)	103.1830(10)	79.2060(10)	62.548(18)
γ (deg)	90	106.681(4)	90	83.8300(10)	84.31(3)
V (Å^3)	2352.87(16)	1297.0(2)	3730.48(18)	2030.70(9)	1981.7(10)
Z	4	2	4	2	2
T (K)	293	293	293	293	293
ρ_{calcd} (g/cm^3)	1.534	1.752	1.495	1.965	1.883
μ (mm^{-1})	6.265	6.960	4.063	7.663	7.745
R [$I_o \geq 2.5\sigma(I_o)$]	0.0293	0.0232	0.0232	0.0331	0.0442
R_w [$I_o \geq 2.5\sigma(I_o)$]	0.0368	0.0296	0.0274	0.0405	0.0622

Table 2. Summary of Crystallographic Data for Compounds **6**−**9**

	trans-[CoCl$_2$(en)$_2$][Au(CN)$_4$] (**6**)	[Ni(en)$_3$][Au(CN)$_4$]$_2$ (**7**)	[Co(NH$_3$)$_6$][Au(CN)$_4$]$_3$·4H$_2$O (**8**)	[Hdabco][Au(CN)$_4$] (**9**)
empirical formula	$C_8H_{16}N_8AuCl_2Co$	$C_{14}H_{24}N_{14}Au_2Ni$	$C_{12}H_{25}N_{18}Au_3CoO_4$	$C_{20}H_{26}N_{12}Au_2$
formula weight	551.07	841.08	1135.28	828.44
crystal system	monoclinic	monoclinic	orthorhombic	monoclinic
space group	$P2_1/a$	$P2_1/c$	$P2_12_12_1$	$P2_1/c$
a (Å)	8.7523(5)	13.865(2)	7.40440(10)	7.1769(3)
b (Å)	8.0191(5)	12.345(2)	18.9411(3)	15.5957(5)
c (Å)	11.7635(8)	16.213(3)	21.4134(3)	12.3167(4)
α (deg)	90	90	90	90
β (deg)	94.729(3)	112.002(2)	90	104.269(2)
γ (deg)	90	90	90	90
V (Å^3)	822.82(9)	2573.0(8)	3003.18(8)	1336.06(8)
Z	2	4	4	2
T (K)	293	293	293	293
ρ_{calcd} (g/cm^3)	2.224	2.171	2.511	2.059
μ (mm^{-1})	10.239	12.129	15.203	11.000
R [$I_o \geq 2.5\sigma(I_o)$]	0.1011	0.0246	0.0220	0.0267
R_w [$I_o \geq 2.5\sigma(I_o)$]	0.1072	0.0266	0.0290	0.0314

Varian ^{UNITY}Inova 600 (B_0 = 14.1T) at 60.81 MHz, using a 3.2 mm double-resonance MAS probe (Varian-Chemagnetics) with a spinning frequency of 10 000 ± 3 Hz and 22 μL (or 36 μL, thin walled) ZrO_2 rotors. CP experiments were acquired on natural abundance samples with 7 to 10 ms contact times, a 4.2 μs excitation pulse on ^{1}H (optimized for the Hartmann−Hahn match), optimized recycle delays between 5 to 40 s, and 8k to 50k coadded transients. Chemical shifts are reported with respect to saturated ammonium nitrate (NH_4^+, 0.0 ppm), using ^{15}N-enriched solid glycine (11.59 ppm) as a secondary reference.[41,42]

Results

Synthesis and Structural Characterization. [^{n}Bu$_4$N][Au(CN)$_4$] (1), [AsPh$_4$][Au(CN)$_4$] (2), [N(PPh$_3$)$_2$][Au(CN)$_4$] (3), [Co(phen)$_3$][Au(CN)$_4$]$_2$ (4), [Mn(terpy)$_2$][Au(CN)$_4$]$_2$ (5). To prepare crystals of **1**, **2**, and **3**, aqueous solutions of [^{n}Bu$_4$N]Br, [AsPh$_4$]Cl, or [N(PPh$_3$)$_2$]Cl, respectively, were added to an aqueous solution of K[Au(CN)$_4$]. Crystals of **4** were prepared by mixing 50% MeOH/H_2O solutions of phen and Co(ClO$_4$)$_2$·6H_2O, followed by addition of two equivalents of KAu(CN)$_4$. Crystals of **5** were prepared by mixing 50% MeOH/H_2O solutions of terpy and $MnCl_2$·6H_2O, followed by addition of an aqueous solution containing two equivalents of KAu(CN)$_4$. For compounds **1**-**5**, once the solutions were mixed, the solvents were allowed to slowly evaporate until crystals suitable for X-ray analysis were deposited, typically taking 1−14 days.

The crystal structures of compounds **1**−**4** show standard, unremarkable bond lengths and angles. The [Au(CN)$_4$]$^-$ anions are well-separated from one another in these compounds; no Au−Au or Au−N interactions are present since the shortest Au−Au distances range from 4.323 to 8.249 Å (well outside the range of Au−Au metallophilic interactions) while the shortest Au···N distances range from 3.266(2) (in **2**) to 6.137(4) Å (Table 3). These Au···N distances are at the limit of or are longer than the sum of the van der Waals radii of Au and N: 3.12−3.27 Å.[43] Only for **5** is weak aggregation of [Au(CN)$_4$]$^-$ anions through very long Au···N interactions observed: weak trans-axial coordination of Au(2) through Au−N interactions results in [Au(CN)$_4$]$^-$ trimers (Au(2)−N(11) = 3.228(17) Å; Table S1) and an octahedral Au(III) center (Supporting Information Figure S1). This Au···N interaction is also longer than for most previously reported compounds, which have been in the range of 2.963(13)−3.3035(8) Å.[35]

(41) Hayashi, S.; Hayamizu, K. *Bull. Chem. Soc. Jpn.* **1991**, *64*, 688–690.
(42) Shoji, A.; Ozaki, T.; Fujito, T.; Deguchi, K.; Ando, S.; Ando, I. *J. Am. Chem. Soc.* **1990**, *112*, 4693–4697.
(43) Bondi, A. *J. Phys. Chem.* **1964**, *68*, 441–451.

Table 3. Comparison of Compounds **1**–**9**, Their Minimum Au–Au Distances, Au–N Distances, and Observed ν_{CN} IR Bands

compound	minimum Au–Au distances (Å)	minimum Au–N distances (Å)	observed ν_{CN} bands in IR (cm^{-1})
$[^nBu_4N][Au(CN)_4]$ (**1**)	8.118	6.137(4)	2183
$[AsPh_4][Au(CN)_4]$ (**2**)	4.342	3.266(2)	2192, 2181, 2179
$[N(PPh_3)_2][Au(CN)_4]$ (**3**)	8.249	5.665(5)	2179
$[Co(phen)_3][Au(CN)_4]_2$ (**4**)	4.815	3.357(6)	2199, 2190, 2185, 2180
$[Mn(terpy)_2][Au(CN)_4]_2$ (**5**)	4.963	3.228(17)	2188
trans-$[Co(en)_2Cl_2][Au(CN)_4]$ (**6**)	5.935	3.072(13)	2186
$[Ni(en)_3][Au(CN)_4]_2$ (**7**)	4.401	3.056(5), 3.082(5)	2185, 2176
$[Co(NH_3)_6][Au(CN)_4]_3\cdot(H_2O)_4$ (**8**)	4.975, 5.099	3.004(6), 3.010(6), 3.022(6), 3.052(7)	2191, 2189
[Hdabco][$Au(CN)_4$] (**9**)	6.158	2.958(6)	2196, 2184, 2175

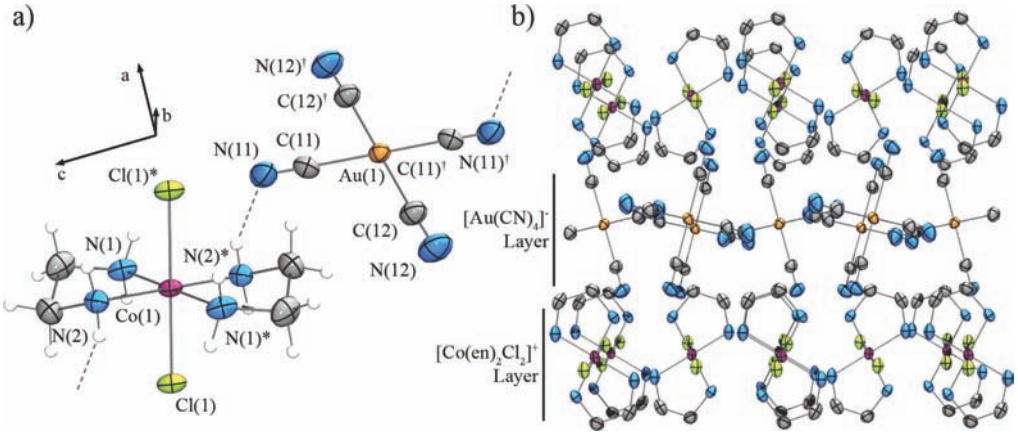

Figure 1. (a) Asymmetric unit of **6** showing the chain formed by hydrogen bonding between N(11)···H(21)*—N(2)* and (b) the view of the solid state crystal viewed down the *a*-axis showing layering that occurs between [*trans*-$Co(en)_2Cl_2]^+$ and $[Au(CN)_4]^-$ ions. Hydrogen atoms are removed for clarity.

[*trans*-Co(en)$_2$Cl$_2$][Au(CN)$_4$] (6). A solution of methanolic *trans*-$[Co(en)_2Cl_2]Cl$ mixed with methanolic $KAu(CN)_4$ deposited green crystals of **6** after four days. The IR spectrum showed a ν_{CN} peak at 2186 cm^{-1}, slightly shifted from the 2183 cm^{-1} of $[^nBu_4N][Au(CN)_4]$ (**1**).

The crystal structure of **6** contains a cobalt(III) cation octahedrally coordinated by chloride and en ligands in a *trans* fashion (Figure 1a). Selected bond lengths and angles are listed in Supporting Information Table S2. Hydrogen bonding occurs between the $[Co(en)_2Cl_2]^+$ and $[Au(CN)_4]^-$ ions, such that the N-cyano end of CN(11) acts as a hydrogen bond acceptor and N(2) acts as a hydrogen bond donor (N(11)···H(21)*–N(2)* = 2.997(17) Å; C(11)–N(11)–N(2)* = 119.6(9)°). This length is consistent with hydrogen bonds previously observed in a similar structural study investigating hydrogen bonding between $[M(NH_3)_6][Au(CN)_2]_x$ salts, which were typically slightly greater than 3.0 Å.[27] Each en ligand is involved in formation of these hydrogen bonds, which are propagated infinitely throughout the crystal and aid the formation of a supramolecular structure where *trans*-$[Co(en)_2Cl_2]^+$ and $[Au(CN)_4]^-$ ions form separate layers (Figure 1b). This type of structure encourages self-aggregation of $[Au(CN)_4]^-$ anions because they are not physically isolated from one another, as found in **1**–**5**.

Indeed, weak Au···NC coordinate bonds are observed between N(12) and Au(1)‡ such that the Au atom is octahedral, but exhibiting a great deal of axial distortion (Au(1)‡–N(12) = 3.072(13) Å; Au(1)‡–N(12)–C(12) = 145.4(13)°). These N-cyano–gold interactions are similar in length to previously described compounds.[35] The N-cyano ends of C(12)†–N(12)† coordinate to adjacent gold atoms, forming a 2-D (4,4) net motif (Figure 2).[17] No

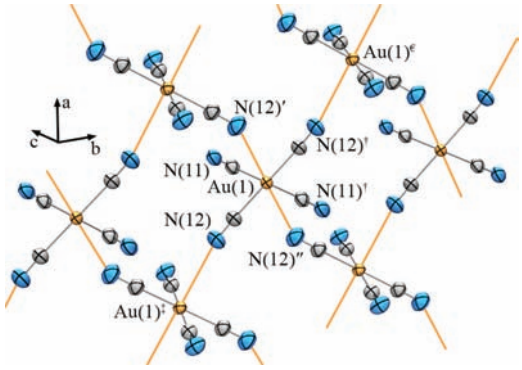

Figure 2. View of the (4,4) $[Au(CN)_4]^-$ net formed by crystallographically equivalent Au···N interactions of 3.072(13) Å in **6**. *trans*-$[Co(en)_2Cl_2]^+$ cations have been removed for clarity.

gold–gold interactions are observed in this structure; hydrogen bonding between the cations and nitriles of the anions, and Au···NC interactions contribute to cation/anion and anion/anion aggregation, respectively.

Some five- and six-coordinate Au(III) complexes are known, although Au(III) is normally square planar.[44] Five-coordinate Au(III) complexes[45,46] typically incorporate a chelating ligand exhibiting some rigidity, such as 2,2′-bipyridine, phenanthroline, or 2,2′:6′:2″-terpyridine, which allows one pyridyl group to coordinate to a basal site on the Au(III) center while the other pyridyl group

(44) Cotton, F. A.; Wilkinson, G. *Advanced Inorganic Chemistry*; 3rd ed.; Interscience: New York, 1972.
(45) Kilpin, K. J.; Henderson, W.; Nicholson, B. K. *Inorg. Chim. Acta* **2009**, *362*, 5080–5084.
(46) Sommerer, S. O.; MacBeth, C. E.; Jircitano, A. J.; Abboud, K. A. *Acta Crystallogr. C* **1997**, *53*, 1551–1553.

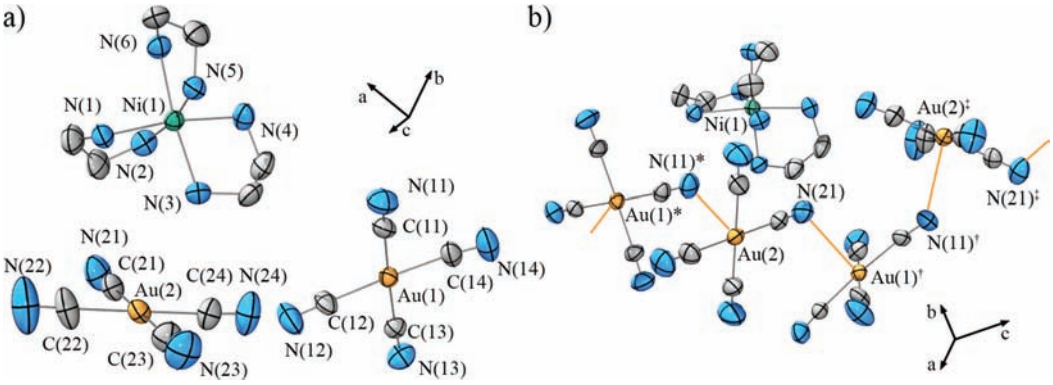

Figure 3. (a) Asymmetric unit of **7** and (b) the 1-D chain formed by intermolecular Au···N interactions. Hydrogen atoms are omitted for clarity.

coordinates to the apical site.[47−51] A six-coordinate Au(III) complex based on a macrocyclic ligand with four equatorial nitrogen donors and axial chloride ligands has been reported; a great disparity in bond lengths is observed between the equatorial and axial ligands (also seen here in **6**), which average 2.049(8) and 3.097(4) Å, respectively.[52]

$[Ni(en)_3][Au(CN)_4]_2$ (7). Mixing an aqueous solution of $[Ni(en)_3]^{2+}$ with $[Au(CN)_4]^-$ resulted in the deposition of large purple crystals of **7**. The IR spectrum of **7** shows ν_{CN} peaks at 2185 and 2176 cm^{-1}.

The X-ray crystal structure of **7** shows an octahedrally coordinated Ni(II) cation, bound by three bidentate en ligands with a Λ stereochemistry and $[Au(CN)_4]^-$ anions (Figure 3a). The Ni(1)−N, Au−C, and C−N bond lengths are unremarkable (Supporting Information Table S3). In the supramolecular structure there is an absence of hydrogen bonding despite the ability of the en amino groups to act as hydrogen bond donors. However, intermolecular Au···N interactions are observed between Au(2) and N(11)* as well as between Au(1) and N(21)′ (Au(2)−N(11)* = 3.056(5) Å; Au(1)−N(21)′ = 3.082(5) Å). These Au···N interactions cause both Au(1) and Au(2) to be five-coordinate, adopting a square pyramidal geometry. However, the apical coordination of both Au(1) and Au(2) only causes slight distortion of the basal CN^- ligands away from planarity for Au(1) and almost no distortion about Au(2) (C(1)−Au(1)−C(3) = 175.39(19)°, C(2)−Au(1)−C(4) = 177.7(2)°; C(5)−Au(2)−C(7) = 179.1(2)°, C(6)−Au(2)−C(8) = 179.7(3)°). These Au···N interactions facilitate formation of $[Au(CN)_4]^-$ 1-D chains in the supramolecular structure, as seen in Figure 3b. The 1-D chains of $[Au(CN)_4]^-$ anions are separated from one another by $[Ni(en)_3]^{2+}$ cations.

$[Co(NH_3)_6][Au(CN)_4]_3 \cdot 4H_2O$ (8). The reaction of aqueous $[Co(NH_3)_6]^{3+}$ and $[Au(CN)_4]^-$ resulted in an orange solution that yielded orange crystals of **8**. The IR spectrum of **8** has two ν_{CN} bands at 2189 and 2191 cm^{-1}. The asymmetric unit of **8** consists of an octahedral hexaamminecobalt(III) cation, three $[Au(CN)_4]^-$ units, and four cocrystallized H_2O molecules (Figure 4a). The bond lengths and angles for the $[Au(CN)_4]^-$ anions are typical (Supporting Information Table S4).

Viewing the supramolecular structure along the *a*-axis reveals alternating layers of $[Co(NH_3)_6]^{3+}$ and $[Au(CN)_4]^-$ ions with the four water molecules lying within the cationic layer (Figure 4b), similar to that observed in **6**. Within the $[Au(CN)_4]^-$ layer in **8**, Au···N interactions are observed between the adjacent $[Au(CN)_4]^-$ anions. There are four crystallographically unique, relatively short Au···N interactions, generating octahedral coordination of Au(2), while Au(1) and Au(3) each display square pyramidal coordination (Au(1)−N(24) = 3.052(7) Å; Au(2)−N(13)′ = 3.010(6) Å, Au(2)−N(31) = 3.022(6); Au(3)−N(34)‡ = 3.004(6) Å). This weak axial coordination has little structural impact on the C-bound CN^- ligands in the equatorial plane. Figure 5 shows the network of aggregated $[Au(CN)_4]^-$ anions.

Hydrogen bonding plays a large role in the packing of **8**; terminal N-cyano units act as hydrogen bond acceptors to both coordinated amine ligands and interstitial water molecules. Hydrogen bonding also facilitates the layering between cations and anions; the terminal N-cyano units all participate in either hydrogen bonds, short Au···N interactions, or weak Au···N contacts slightly longer than 3.27 Å.

[Hdabco][Au(CN)$_4$] (9). Mixing aqueous solutions of [Hdabco]Cl and K[Au(CN)$_4$] resulted in crystals of **9**. The IR spectrum showed the presence of C−H bonds attributable to the dabco ligand and ν_{CN} modes at 2196 and 2184 cm^{-1}. The crystal structure of **9** consists of the $[Hdabco]^+$ cation and two $[Au(CN)_4]^-$ anions (Figure 6a). A hydrogen bond is present between the protonated amine of the $[Hdabco]^+$ cation, N(2), and the N(11)-cyano unit of Au(1) (Figure 6, N(11)···H(23)−N(2) = 2.869(5) Å, C(11)−N(11)···H(23)−N(2) = 162.3(3)°). This hydrogen bond is substantially shorter than those seen in **6** (2.997(17) Å). The crystallographically equivalent trans N(11)−C(11) unit also participates in an equivalent hydrogen bond, such that each Au(1) $[Au(CN)_4]^-$ anion bridges two $Hdabco^+$ cations through hydrogen bonding. Selected bond lengths and angles are collected in Supporting Information Table S5.

In addition to the hydrogen bonding, two $[Hdabco]^+$ cations coordinate to the vacant axial sites of Au(1)

(47) Cinellu, M. A.; Zucca, A.; Stoccoro, S.; Minghetti, G.; Manassero, M.; Sansoni, M. *J. Chem. Soc., Dalton Trans.* **1996**, 4217–4225.
(48) Ferretti, V.; Gilli, P.; Bertolasi, V.; Marangoni, G.; Pitteri, B.; Chessa, G. *Acta Crystallogr. C* **1992**, *48*, 814–817.
(49) Marangoni, G.; Pitteri, B.; Bertolasi, V.; Gilli, G.; Ferretti, V. *J. Chem. Soc., Dalton Trans.* **1986**, 1941–1944.
(50) O'Connor, C. J.; Sinn, E. *Inorg. Chem.* **1978**, *17*, 2067–2071.
(51) Vicente, J.; Chicote, M. T.; Bermudez, M. D.; Jones, P. G.; Fittschen, C.; Sheldrick, G. M. *J. Chem. Soc., Dalton Trans.* **1986**, 2361–2366.
(52) Suh, M. P.; Kim, I. S.; Shim, B. Y.; Hong, D.; Yoon, T. S. *Inorg. Chem.* **1996**, *35*, 3595–3598.

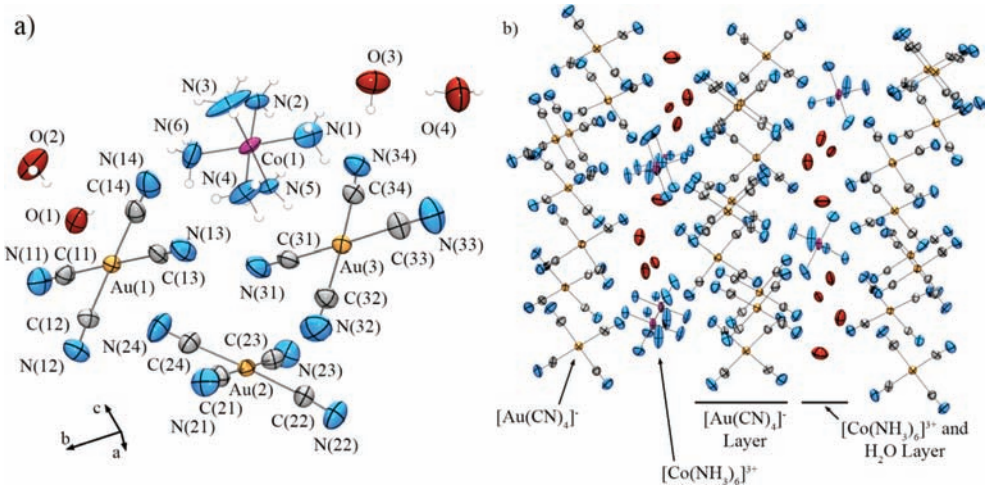

Figure 4. (a) Asymmetric unit of $[Co(NH_3)_6][Au(CN)_4]_3 \cdot 4H_2O$ (**8**) and (b) a view of the packing in the crystal structure, while looking down the *a*-axis, showing layers of $[Au(CN)_4]^-$ anions alternating with layers of $[Co(NH_3)_6]^{3+}$ cations and water molecules. Hydrogen atoms in b are removed for clarity.

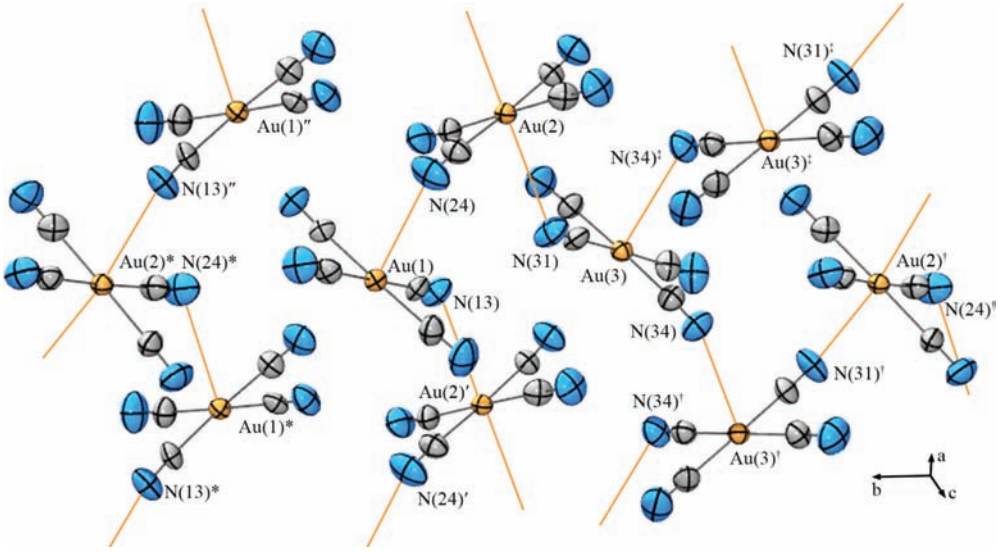

Figure 5. Network of $[Au(CN)_4]^-$ anions formed by Au···N interactions in **8**.

through an unprotonated amine, N(1). Thus, Au(1) is formally octahedral, with a large axial elongation (Au(1)−N(1)″ = 2.932(2) Å). It is worth noting that this Au···N interaction is shorter than the Au···NC−Au interactions observed in **6**−**8**, suggesting that the alkyl amine group of the $[Hdabco]^+$ ligand is more Lewis-basic than the terminal N-cyano groups of $[Au(CN)_4]^-$. The hydrogen bonds and long gold-amine coordinate bonds propagate chains of $[Hdabco]^+$ and $[Au(CN)_4]^-$ in two dimensions, thereby forming a (4,4) net (Figure 6b).[17] The anion containing Au(2) lies in the open spaces formed by this net and does not participate in hydrogen bonding or Au−N interactions. Adjacent nets pack with weak van der Waals forces; there do not appear to be any gold−gold or Au···N interactions supporting packing between layers.

Correlation of Structural and IR Spectral Features. The identification and characterization of a weak intermolecular bonding interaction in coordination polymers often relies predominantly on a distance argument, that is, if the atoms in question lie within a certain threshold (e.g., the sum of the van der Waals radii) in the X-ray crystal structure, then the interaction is considered to be significant. Given the limitations of such an analysis, especially when the interaction in question (Au···NC) has relatively few crystallographic examples overall, independent (nonstructural) spectroscopic evidence for the significance of such an interaction is invaluable. With this in mind, Table 3 compares **1**-**9** by their shortest Au−Au distances, Au···N distances (or length of Au···N interactions, where appropriate), and observed ν_{CN} bands in the infrared spectra. IR spectroscopy is normally very useful in identifying bridging of cyanometallate-containing compounds based on red- or blue-shifting of the ν_{CN} mode.[18] $KAu(CN)_4$ has a ν_{CN} band at 2189 cm^{-1}, while **1** and **3** have weak ν_{CN} resonances at 2183 and 2179 cm^{-1} respectively; these latter compounds have only well-isolated N-cyano units (crystallographically), suggesting that any substantial shifting from these values could provide a good spectroscopic signature for bridging, intermolecular Au···NC units. Curiously, **2** and **4** also both show ν_{CN} modes at roughly 2180 cm^{-1}, along with

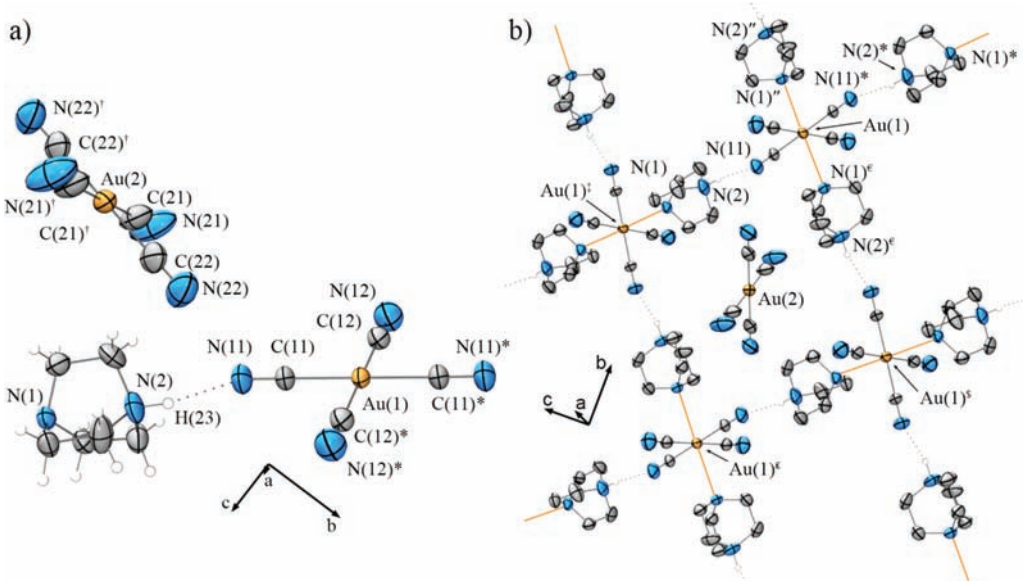

Figure 6. (a) The asymmetric unit of **9**. In (b), $[Au(CN)_4]^-$ and $Hdabco^+$ ions form an extended network through hydrogen bonding and Au···N interactions.

additional blue-shifted peaks that suggest that some N-cyano units are bridging rather than terminal, despite X-ray evidence to the contrary. Furthermore, the IR spectrum of **5** has a single ν_{CN} mode at 2188 cm^{-1}, the blue-shifting of which normally suggests that the N-cyano units in this structure may be exclusively bridging to another metal. Even though it should be recognized that the ν_{CN} values for compounds **1**−**5** are all between the fairly small range of 2179−2188 cm^{-1} (Table 3), overall, there appears to be no trend in the ν_{CN} values that correlates readily with Au···NC distances.

The apparent contradictions between the structural features of **1**−**5** and their IR spectra show that it is difficult to make structural assertions based on the IR spectra for $[Au(CN)_4]^-$-containing compounds. Thus, the ν_{CN} values appear to be a poor indicator of the presence or absence of N-cyano bridging between metals; this may be partly because of the very low intensity of the observed bands. It is worth noting that the weak peaks inherent to $[Au(CN)_4]^-$, as previously noted by others,[35,36] confound IR analysis such that identification of peaks is much more difficult than in cyanometallates with strongly absorbing ν_{CN} bands such as $[Au(CN)_2]^-$ or $[Pt(CN)_4]^{2-}$.[18,53] In this light, we turned to solid-state ^{15}N MAS NMR as a potential tool to shed spectroscopic insight on the Au···NC interactions that were observed crystallographically.

Nitrogen-15 CP MAS NMR. The nitrogen-15 isotropic chemical shift has been shown to be sensitive to three types of cyanide interactions observed in metal-cyanide complexes: C-bound terminal, bridging, and N-bound terminal cyanide ligands.[54,55] Terminal C-bound cyanide ligands are observed in the high ^{15}N chemical shift range from 260 to 320 ppm.[55] Bridging cyanides, where the nitrogen on the cyanide ligand (i.e., the N-cyano unit) is in close proximity to an electron-donating atom (often other metals, e.g., Zn, Hg, Au), occur in an intermediate ^{15}N chemical shift range of 225−255 ppm. N-bound terminal cyanides have the lowest chemical shifts. For example, AuNC has a ^{15}N chemical shift of ~200 ppm.[54] Figure 7 illustrates that these regions can be used as a rough "fingerprint" for determining cyanide speciation.[34,54−58]

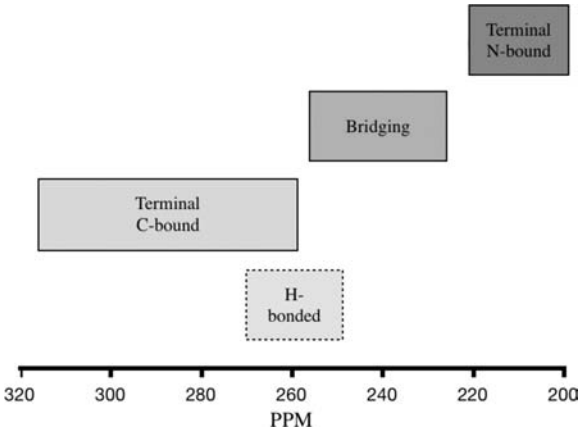

Figure 7. Approximate ^{15}N NMR chemical shift regions for cyanide groups from this and previous studies.[34,54−58]

$^{15}N\{^1H\}$ CP-MAS NMR of the natural abundance samples reveals well-defined, ordered cyanide groups in the six diamagnetic compounds (**1**−**3**, **6**, **8**, **9**, see Table 4) with chemical shifts in the range expected for C-bound ligands (320−260 ppm).[55,61] Compounds **1**, **2**, and **3** each

(53) Nakamoto, K. *Infrared and Raman Spectra of Inorganic and Coordination Compounds*; 5th ed.; John Wiley & Sons: New York, 1997.
(54) Harris, K. J.; Wasylishen, R. E. *Inorg. Chem.* **2009**, *48*, 2316–2332.
(55) Schwarz, P.; Siebel, E.; Fischer, R. D.; Davies, N. A.; Apperley, D. C.; Harris, R. K. *Chem.—Eur. J.* **1998**, *4*, 919–926.
(56) Kroeker, S.; Wasylishen, R. E.; Hanna, J. V. *J. Am. Chem. Soc.* **1999**, *121*, 1582–1590.
(57) Bryce, D. L.; Wasylishen, R. E. *Inorg. Chem.* **2002**, *41*, 4131–4138.
(58) Al-Maythalony, B. A.; Fettouhi, M.; Wazeer, M. I. M.; Isab, A. A. *Inorg. Chem. Commun.* **2009**, *12*, 540–543.
(59) Juranic, N.; Lichter, R. L. *J. Am. Chem. Soc.* **1983**, *105*, 406–410.
(60) Gobetto, R.; Nervi, C.; Valfre, E.; Chierotti, M. R.; Braga, D.; Maini, L.; Grepioni, F.; Harris, R. K.; Ghi, P. Y. *Chem. Mater.* **2005**, *17*, 1457–1466.
(61) Pines, A.; Gibby, M. G.; Waugh, J. S. *J. Chem. Phys.* **1973**, *59*, 569–590.

Table 4. ^{15}N NMR Isotropic Chemical Shifts for $Au(CN)_4^-$ Salts

cmpd	name	^{15}N chemical shifts (±2 ppm, unless otherwise indicated)				nitrogen site (number of crystallographically inequivalent sites)	
1	$[^nBu_4N][Au(CN)_4]$	275	46.4[a]			CN(4)	$Bu_4N(1)$
2	$[AsPh_4][Au(CN)_4]$	270				CN(4)	
3	$[N(PPh_3)_2][Au(CN)_4]$	272				CN(4)	PPN(1)
6	$[Co(en)_2Cl_2][Au(CN)_4]$	264.3(5)	257.2(5)	−30[b]		CN(2)	en(2)
8	$[Co(NH_3)_6][Au(CN)_4]_3\cdot(H_2O)_4$	258				CN(12)	$NH_3(6)$
9	[Hdabco][$Au(CN)_4$]	270(1)	250(1)	19[c]	−12.7[c]	CN(4)	Hdabco(2)

[a] $^nBu_4N$.[55] [b] en.[59] [c] Hdabco.[60]

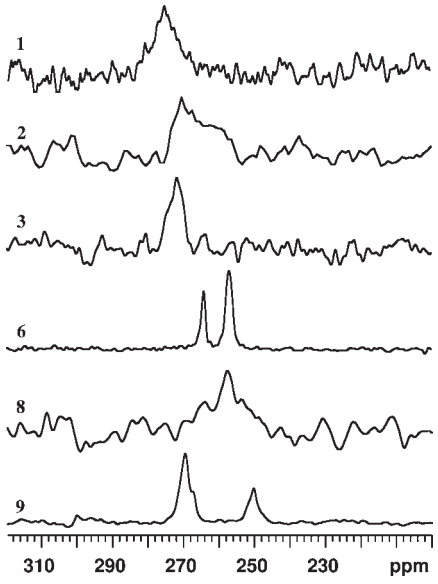

Figure 8. ^{15}N chemical shifts of the cyanide region for diamagnetic $[Au(CN)_4]^-$ salts.

feature a single broad peak between 260 and 275 ppm, representing the overlap of unresolved crystallographically inequivalent cyanides in structurally similar terminal environments (Figure 8). Compound **9** yields a narrower composite peak at ca. 270 ppm constituting 75% of the signal, which can be assigned to the three terminal cyanides. Likewise, **6** possesses two cyanide species, one of which appears at 264 ppm and represents the terminal cyanide. Compounds **6**, **8**, and **9** contain H-bond donating ligands and crystallographic evidence of CN···H−N bonding. Each of these spectra exhibits peaks at lower chemical shifts (250−257 ppm), consistent with previous work indicating that hydrogen bonding induces a shift to lower ^{15}N frequencies.[55,62] For example, CN···H−O bonding in a series cobalt cyanide compounds reduces the shift range by about 15−20 ppm with respect to terminal cyanides.[55] Compounds **6** and **8** also contain terminal cyanides without H-bonding which appear around 264 and 270 ppm, respectively. Hence, gold-bound cyanides have a ^{15}N chemical shift region between 260 and 275 ppm that can be assigned to C-bound terminal ligands, while those subject to N···H−N bonding resonate in a lower frequency chemical shift region of 250−257 ppm.

There also appears to be a relationship between the ^{15}N chemical shift and Au−N distances. In **1** and **3**, where the nearest Au−N distances are all very long (5.66−11.12 Å), the chemical shifts are at or above 270 ppm. In **2**, there is a range of Au−N distances from the relatively short 3.27 Å, through the intermediate distance of 4.12 Å, to two distances greater than 9 Å. The corresponding peak is broad, with greatest intensity around 270 ppm and significant intensity as low as 260 ppm, implying that the shortest Au−N distances are shifted to lower frequency. The non-H-bonded peak in **6** has a very short Au−N distance of 3.07 Å and its shift of 264 ppm is quite low relative to the others. Likewise, **9** shows evidence of two distinct resonances around 270 ppm: the peak with the strongest intensity appears at the highest frequency and likely corresponds to the two cyanides with the longest Au−N distances (4.93 and 5.25 Å), while the lower frequency shoulder with half the intensity can be assigned to the cyanide with a Au−N distance of 3.51 Å. Compound **8** has 12 inequivalent cyanides with a wide range of Au−N distances, but its shift(s) is dominated by extensive hydrogen-bonding. Hence, while the primary influence on ^{15}N chemical shifts in this system is the well-known effect of hydrogen-bonding, it appears that closer proximity to Au shifts the ^{15}N peaks to low frequency, a correlation which can be used for peak assignments and possibly for the determination of unknown structures. In a general sense, it is clear that, for the first time, there is a real, spectroscopically measurable electronic effect associated with the crystallographic observation of intermolecular Au···NC interactions, thereby lending support for their chemical significance.

Discussion

Structural patterns in **1**−**9** agree with previously reported $[Au(CN)_4]^-$-based compounds,[33−35] which indicate self-aggregation of $[Au(CN)_4]^-$ in the solid state appears to rely on Au···N rather than aurophilic interactions. This preference may be due to the Lewis acidity of Au(III) relative to the isoelectronic $[Pt(CN)_4]^{2-}$ (for which metallophilic interactions are common). In turn, the Lewis basic N-cyano groups may bind to the Au(III) centers by coordination to vacant axial sites. Another contributing factor is likely the fact that (because of the higher oxidation state), the Au-based orbitals that would be needed for Au(III)−Au(III) bonding are contracted relative to the Pt(II) analogues. Indeed, only very weak-field ligands are found to support Au(III)-based metallophilicity: such Au(III)−Au(III) aurophilic interactions have been observed only in $[N(CH_3)_4][Au(N_3)_4]$ and $[Au(bipy)Cl_2][AuBr_4]$ (bipy = 2,2′-bipyridine), with (long) Au−Au bond lengths of 3.507(3), 3.508(3), and 3.584(3) Å for the former compound and 3.518(1) Å for the latter;[63,64]

(62) Lorente, P.; Shenderovich, I. G.; Golubev, N. S.; Denisov, G. S.; Bunthowsky, G.; Limbach, H.-H. *Magn. Reson. Chem.* **2001**, *39*, S18–S29.

(63) Hayoun, R.; Zhong, D. K.; Rheingold, A. L.; Doerrer, L. H. *Inorg. Chem.* **2006**, *45*, 6120–6122.

(64) Klapötke, T. M.; Krumm, B.; Galvez-Ruiz, J. C.; Nöth, H. *Inorg. Chem.* **2005**, *44*, 9625–9627.

both sets of distances are still relatively long compared to those observed for Au(I), which are frequently shorter than 3.1 Å.[20]

In this study, the cations were judiciously chosen to provide comparisons between $[Au(CN)_4]^-$-containing compounds based on the variations in shape, charge (+1 or +2) and the presence or absence of groups with available π-systems, as well as their abilities to participate in H-bonding. Among all of these factors, from examining the summary of Au···N distances in Table 3 and utilizing the sum of the van der Waals radii limit for Au and N (3.27 Å) as a cutoff, it is clear that Au···NC interactions are much shorter when the countercation is capable of participating in hydrogen bonding with terminal N-cyano units of the $[Au(CN)_4]^-$ anion.

Thus, compounds **6**−**9**, where the cation is a hydrogen bond donor, all exhibit significant Au···N interactions in the solid state, ranging from 2.958(6) to 3.082(5) Å (Table 3). Most of these compounds (except $[Ni(en)_3][Au(CN)_4]_2$) show terminal N-cyano groups participating in hydrogen bonding to the cation, which acts to withdraw electron density from the $[Au(CN)_4]^-$ molecule to some degree. Formation of this hydrogen bonding may increase the Lewis acidity of the Au(III) center, making intermolecular Au···N interactions more favorable.

In **9**, hydrogen bonds are formed between the protonated aliphatic amine of $[Hdabco]^+$ and the terminal N-cyano groups. As a result, long axial binding to the central Au(III) atom is observed through the unprotonated aliphatic amine from $[Hdabco]^+$. This appears to be a more favorable Au···N interaction that would be formed by coordination of a terminal N-cyano group, as the free $[Au(CN)_4]^-$ molecule remains in the interstitial spaces of the network. This preference suggests that, unsurprisingly, the dabco amine group is more basic than the N-cyano units of $[Au(CN)_4]^-$.

Previously synthesized coordination polymers employing $[Au(CN)_4]^-$ have also shown a number of Au−N interactions ranging in length from 2.963(13) to 3.052(9) Å, slightly shorter than in **6**−**9**.[35] Their presence can be rationalized in a similar fashion: binding of the N-cyano group to a metal cation redistributes the electron density from Au(III) to the metal cation, thereby increasing the Lewis acidity of the Au(III) center and promoting intermolecular Au···N interactions. Thus, in addition to hydrogen bonding, it appears that the generation of Au(III)−CN−M bridges in coordination polymers is also favorable to formation of intermolecular Au···N interactions.

On the other hand, cationic charge does not appear to play a role in inducing the formation of Au···N interactions. This assessment is based on comparing structures with steric, noncoordinating, monovalent cations in **2** and **3** versus bulky, divalent cations in **4** and **5**. Au···N interactions are absent in all of these structures (with the exception of the marginal ones in **5**). This suggests that self-aggregation is only very slightly influenced by cationic charge for cations with a relatively uniform electronic topology, such as those with large aromatic or aliphatic groups. This interpretation of the (minimal) effect of cation charge on Au···N interaction formation is also consistent with the series of structures that contain hydrogen bonding cations (**6**−**9**) in that there is no trend in the Au···N distances that would suggest that the presence or strength of the observed Au···N interactions depend on the relative number of $[Au(CN)_4]^-$ anions.

Similarly, the shape and aromaticity of the cations appears to play a minimal, if any, role in self-aggregation of $[Au(CN)_4]^-$ anions. Compounds **1**-**3** differ by the shape of, and ability to $\pi-\pi$ stack their aromatic groups in, their respective cations, but nonetheless the $[Au(CN)_4]^-$ anions are isolated from one another in all three structures.

Conclusions

The series of solid-state structures of $[Au(CN)_4]^-$ containing salts illustrate that when N-cyano units bridge the central Au(III) atom and another group (be it a metal cation or H-bond), the Lewis acidity of the central Au(III) appears to increase, which induces self-aggregation of the $[Au(CN)_4]^-$ anions by intermolecular Au···NC interactions; no aurophilic interactions are observed. The distances of the N-cyano ligands to the vacant Au(III)-axial sites are long, but within the sum of the van der Waals radii. In addition to the crystallographic evidence, ^{15}N CP MAS NMR data provide solid corroboration in support of the existence of Au···NC interactions. The combination of the ^{15}N chemical shifts for CN^- units presented herein and those of previously published works reveal distinct ranges which may serve to distinguish among various metal-cyanide interactions in unknown structures. Thus, the designed incorporation of hydrogen bond donor groups into the cation is a viable route to increasing the dimensionality of $[Au(CN)_4]^-$ based materials via Au···N interactions, while the cationic charge, shape, size, and aromaticity of the cation do not appear to have an appreciable effect on the ability of $[Au(CN)_4]^-$ molecules to form Au···N interactions.

Acknowledgment. We are grateful to NSERC of Canada (D.B.L., S.K.), the World Gold Council GROW program (D.B.L.), the Natural Resources Canada Internship program (A.R.G.), and a Grant-in-Aid for Scientific Research (A) (No. 17205008) from the Ministry of Education, Culture, Sports, Science, and Technology of Japan (K.S.) for financial support. V.K.M. is grateful to NSERC for a postgraduate scholarship. Infrastructure support from the Canada Foundation for Innovation and the Manitoba Research Innovation Fund (S.K.) is gratefully acknowledged. D.B.L. was generously supported by a JSPS Long-term Invitation Fellowship for 10 months while on sabbatical with his gracious host K.S.

Supporting Information Available: Crystallographic data in cif format for compounds **1**−**9**, additional figures (5), and tables of bond lengths/angles for **5**−**9**. This material is available free of charge via the Internet at http://pubs.acs.org.